

# One-Step Preparation of Highly Dispersed Supported Rhodium Catalysts by Low-Temperature Organometallic Chemical Vapor Deposition

Philippe Serp,\* Roselyne Feurer,† Roland Morancho,† and Philippe Kalck\*,<sup>1</sup>

\*Laboratoire de Chimie des Procédés and †Laboratoire de Cristallographie, Réactivité et Protection des Matériaux, URA-CNRS 445, Ecole Nationale Supérieure de Chimie de Toulouse, 118 Route de Narbonne, 31 077 Toulouse Cedex, France

Received January 20, 1995; revised May 10, 1995; accepted July 25, 1995

A novel method for preparing supported rhodium catalysts using organometallic chemical vapor deposition (OMCVD) has been developed. Vapor of a rhodium complex is brought into contact with silica in a fluidized bed in a special reactor designed to work under reduced pressure (50–100 Torr). Introduction of small amounts of dihydrogen allows rhodium to be deposited at low temperature (100°C); small aggregates (1–2 nm) and high dispersions (0.95–0.70) are obtained. Three convenient precursors,  $[\text{Rh}(\mu\text{-Cl})(\text{CO})_2]_2$ ,  $[\text{Rh}(\eta^3\text{-C}_3\text{H}_5)_3]$ , and  $[\text{Rh}(\text{acac})(\text{CO})_2]$ , have been used, owing to their suitable vapor pressures under experimental conditions. Physicochemical investigations have shown that such deposits are characterized by pure, crystallized rhodium particles. X-ray photoelectron spectroscopy experiments carried out on planar supports (substrates) confirmed the presence of Rh(0) on the surface; near the interface, Rh(I) and Rh(III) centers have been detected, presumably covalently bound to the support. Several homogeneous as well as heterogeneous steps in the reaction mechanism have been shown to be present by monitoring the deposition by mass spectrometry and by infrared spectroscopy. These catalysts display a greater activity for hydrogenation than the corresponding catalysts prepared by the conventional impregnation procedure. © 1995 Academic Press, Inc.

## INTRODUCTION

Usually, impregnation is the main way to prepare supported metal catalysts, but this method requires several steps including reductions and oxidations at high temperatures. Generally, such methods provide dispersions around 0.6 and aggregate sizes near 3 nm. Recently methods (1–7) have been developed for the preparation of smaller particle sizes. For instance, decomposition of fullerene rhodium complexes at 550°C gives rise to very small crystallites of composites containing large amounts of rhodium (1). Photodecomposition of rhodium complexes in solution can

lead to well-dispersed rhodium particles (2–4 nm) on silica or  $\beta\text{-FeOOH}$  supports with loads near 2% w/w (2). Arai *et al.* (3) have investigated the use of sodium tetrahydroborate solutions at room temperature to reduce platinum precursors dispersed on alumina. They report a  $\text{Pt}/\text{Al}_2\text{O}_3$  catalyst with particle sizes near 1 nm.

We have investigated the potentiality of the organometallic chemical vapor deposition (OMCVD) method for the preparation of noble-metal-supported catalysts from suitable precursors (8). Very recently, three papers have appeared describing a two-step preparation of catalytic materials. Dossi and co-workers (9, 10) have prepared some Pd and Pt/zeolite catalysts. The decomposition temperature of the precursors ranged between 100 and 280°C and the size of the metallic particles was reported to be 1.5 nm. It was also shown that  $[\text{Ni}(\text{CO})_4]$  can be deposited on activated carbon in a fluidized bed and in a second step can be decomposed at 250°C in a dinitrogen atmosphere; very large particles were obtained by this process (11). In a similar way, Köhler *et al.* (12) have obtained Pt/SiO<sub>2</sub>, Pt/Al<sub>2</sub>O<sub>3</sub>, or Pt/TiO<sub>2</sub> catalysts starting from  $\text{Pt}(\text{acac})_2$ , with dispersions ranging from 0.4 to 0.7 depending on the nature of the support and the metal loading.

Our objective was to obtain highly dispersed crystallites having a very small size and corresponding to 1–2% supported rhodium (w/w). We have produced deposits, whose full characterization is reported, that consist of 1- to 2-nm-sized particles, corresponding to dispersions of 0.7–0.95.

## EXPERIMENTAL

### Supported Rhodium

The silica support (Sipernat 22), generously provided by Degussa, was sieved between 100 and 200  $\mu\text{m}$  in order that the fluidized bed should be as homogeneous as possible.

The rhodium complexes were prepared according to the published procedures (13, 14) for  $[\text{Rh}(\eta^3\text{-C}_3\text{H}_5)_3]$

<sup>1</sup> To whom correspondence should be addressed.

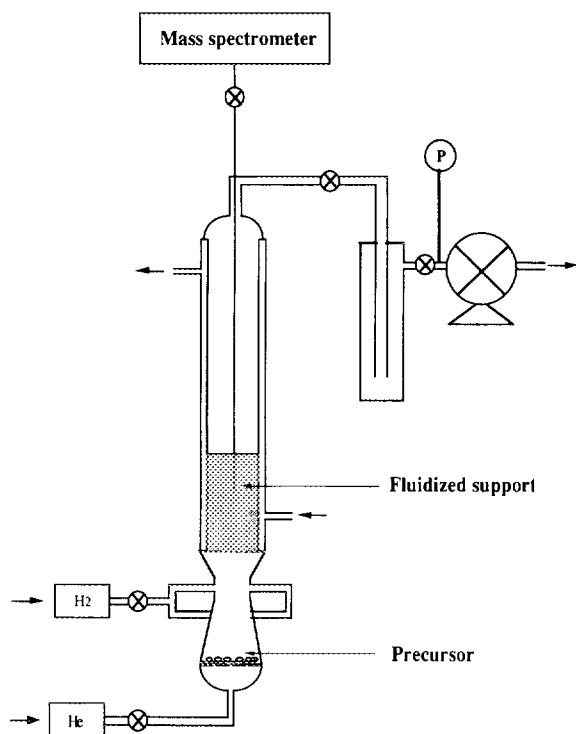


FIG. 1. Schematic diagram of the reactor.

(denoted **2**) and  $[\text{Rh}(\text{CO})_2(\text{acac})]$  (denoted **3**) and according to a new method developed in the laboratory for  $[\text{Rh}_2(\mu\text{-Cl})_2(\text{CO})_4]$  (denoted **1**). Carbon monoxide was bubbled in a solution of 80 ml of methanol containing 4 g of  $\text{RhCl}_3 \cdot 3\text{H}_2\text{O}$  at  $65^\circ\text{C}$ . The red solution gradually turned pale yellow. The reaction, which generally requires 15 h, was monitored by infrared spectroscopy and was stopped as soon as the  $\nu_{\text{CO}}$  band of  $[\text{RhCl}_4(\text{CO})(\text{MeOH})]^-$  at  $2105\text{ cm}^{-1}$  disappeared completely and only the two  $\nu_{\text{CO}}$  bands of  $[\text{RhCl}_2(\text{CO})_2]^-$  at 2070 (vs) and 1994 (vs)  $\text{cm}^{-1}$  were present in the infrared spectra. Then the heating was stopped and methanol was evaporated by introducing a gentle stream of dinitrogen. Complex **1** was formed with very small amounts of black rhodium. Dissolution in hexane and crystallization at  $-25^\circ\text{C}$  produced **1** with a 90% yield. We observed that use of ethanol (15) led to greater amounts of black rhodium at the expense of reduced yield.

The general procedure for preparing Rh/silica catalysts is the following. A mass  $M_a$  of the rhodium complex was introduced as a powder in the sublimator (Fig. 1), where helical shells of glass were added to obtain a good carrier gas/solid exchange area. A mass  $M_s$  of grains of support (silica, for instance) was poured into the column.

The apparatus was placed under reduced pressure (0.1 Torr; 1 Torr =  $133.33\text{ N m}^{-2}$ ) for 1 h. The temperature of the bed was maintained at  $100^\circ\text{C}$  to remove the water

physisorbed on the support; the temperature of the sublimator was kept at  $0^\circ\text{C}$ . Then the bed was heated to temperature  $T_b$  and the pressure in the column was adjusted to the value  $P_a$  by the introduction of the carrier gas. The sublimator was plunged into a warm bath at temperature  $T_s$  and the gas flows ( $Q_v$  for the carrier gas and  $Q_a$  for the reactive gas) were adjusted, a dynamic vacuum being maintained to keep the pressure at the value  $P_a$ . The deposition and the experiment duration was  $t_d$ . The molar ratio of the sublimated precursor to the total gas was  $x$ . At the end of the deposition, the temperature was slowly decreased (1 h) to ambient conditions. The vacuum and the gas flows were stopped and a slow dinitrogen or air stream (25 sccm) was flowed into the apparatus until it reached the ambient pressure. The nonsublimated precursor was recovered. The catalyst was removed from the column and was used without any further treatment.

As an example, a 1% Rh/SiO<sub>2</sub> catalyst was prepared from complex **1** with the following parameters:  $M_a = 1\text{ g}$ ,  $M_s = 5\text{ g}$ ,  $T_b = 100^\circ\text{C}$ ,  $T_s = 52^\circ\text{C}$ ,  $P_a = 50\text{ Torr}$ ,  $Q_v = 35\text{ sccm}$ ,  $Q_a = 8.5\text{ sccm}$ ,  $t_d = 2.5\text{ h}$ , and  $x = 9 \times 10^{-4}$ .

#### Vapor Pressure Measurements

The apparatus for the measurement of the vapor pressures of solids having a low volatility by a static method in the range  $10^{-2}$ –100 Torr and  $30$ – $300^\circ\text{C}$  is described elsewhere (16). The method consists in inserting a membrane, maintained in equipressure by a suitable control loop between the pressure gauge and the product to be tested.

#### Determination of the Rhodium Content

After dissolution of rhodium in aqua regia, the rhodium content of the samples was measured by both atomic absorption spectrophotometry (Perkin–Elmer 3050) and ICP (Spectrometer IL 100). All these analyses were carried out by the Comptoir Lyon-Alemand-Louyot. Results obtained by these two methods were in good agreement.

#### Surface Area and Chemisorption Measurements

Surface area (BET) measurements were performed on an automatic Coultronic apparatus (Accusorb 2100E) monitored by a Hewlett–Packard computer (HP86B). Analyses (50 mg powder) were made by measurement of the gas volume ( $\text{N}_2$ ) adsorbed on the powder.

Chemisorption measurements were carried out using the equipment already described (17, 18). Although the stoichiometric ratio of one CO per rhodium atom, as generally assumed, is not rigorously exact for particle sizes below 2 nm, the results for mean particle size obtained by chemisorption using this assumption are in good agreement with the TEM micrographs.

*Electron Microscopy (SEM/EDS and CTEM/EDS),  
XPS Analysis, and X-ray Analysis*

Scanning electron microscopy (SEM) and conventional transmission electron spectroscopy (CTEM) were performed on Jeol JMS 6400 and TEMSCAN TEST 2010 microscopes, respectively. EDS analyzers were a Link EXL and a TRACOR (Voyager) for the SEM and CTEM, respectively. For the transmission electron microscopy examinations, the samples were dispersed by sonication in ethanol and deposited on a carbon film supported on a copper grid.

X-ray photoelectron spectra were obtained on a VG ESCALAB MK II spectrometer. The measurements were carried out using unmonochromatized  $MgK\alpha$  radiation ( $\lambda = 0.989$  nm) under a mean pressure of  $6 \times 10^{-11}$  kPa.

X-ray diffraction measurements were made on a Seifert XRD 3000 spectrometer using  $CuK\alpha$  radiation ( $\lambda = 0.15406$  nm).

*Catalytic Tests*

The catalytic hydrogenation of benzene was performed in a 100-ml autoclave equipped with a ballast to maintain a constant pressure in the reactor ( $H_2$  total pressure, 2 MPa at  $85^\circ C$ ). Typically, the reactor was charged with 0.29 mol of benzene in 50 ml of ethanol and 1 g of 1% Rh/ $SiO_2$  prepared by the CVD method (7.8 mg of Rh exposed if we take account of a 0.78 dispersion) or 1 g of 1% Rh/ $SiO_2$  prepared by impregnation (6.1 mg of Rh exposed). The products were analyzed by GC/MS (Perkin-Elmer QMASS 910). The conventional 1% Rh/ $SiO_2$  was prepared by impregnation of Degussa Sipernat 22  $SiO_2$  with an aqueous solution of  $RhCl_3 \cdot 3H_2O$ . The sample was dried at  $110^\circ C$ . It was then calcined at  $400^\circ C$  for 10 h and was reduced with  $H_2$  at  $200^\circ C$  for 10 h.

## RESULTS AND DISCUSSION

A fluidized bed reactor was built to handle rhodium complexes without any special precaution. It allows the production of the catalyst in a one-step process. A fluidized bed appeared to be the most suitable way to obtain homogeneous deposits, and owing to the vapor pressure of the rhodium precursors, the experiments were carried out under low pressures (50–100 Torr). Figure 1 shows a schematic diagram of the reactor.

*Selection of the Precursors*

In order to have a general method for depositing rhodium on various supports, the prerequisites for the precursors were that the complexes be stable at room temperature, not be very air-sensitive, be volatile enough, and be selectively decomposed to pure rhodium metal.

From our own experience and from results in the literature (19–22) we studied three compounds:  $[Rh_2(\mu-Cl)_2(CO)_4]$ , **1**;  $[Rh(\eta^3-C_3H_5)_3]$ , **2**; and  $[Rh(acac)(CO)_2]$ , **3**. The vapor pressures of these three solids have been determined as functions of the temperature. In the sublimator, the temperatures have been optimized between 40 and  $55^\circ C$  to provide vapor pressures from 0.05 to 0.08 Torr, without any decomposition.

Similarly, the temperatures of decomposition of these rhodium precursors in the fluidized bed were optimized. It is useful to have a minimal difference between the sublimation and the decomposition temperatures, and to use a temperature such that decomposition occurs completely and very quickly in the bulk of the fluidized bed. Decomposition experiments have been carried out under pure He or  $H_2/He$  mixtures.

Thermolysis of these precursors was monitored by the loss of the various ligands as followed by infrared spectroscopy. Under a  $H_2/He$  atmosphere the best compromise for a complete decomposition was achieved between 80 and  $100^\circ C$ . If the experiments are carried out in the absence of dihydrogen, it is necessary to employ higher temperatures (125, 100, and  $130^\circ C$  for **1**, **2**, and **3**, respectively). The presence of small amounts of dihydrogen in the helium carrier gas allows the decomposition to begin at 75, 65, and  $85^\circ C$  for **1**, **2**, and **3**, respectively. These temperatures are significantly lower than those used by Kumar and Puddephatt (19) for compounds **1** and **2** ( $180^\circ C$ ) to produce rhodium films on silicon wafers; those authors did not find any effect of dihydrogen for **1**. The main difference between the two experimental conditions is the introduction of dihydrogen directly on the rhodium complex by Kumar and Puddephatt (19), whereas we introduce a low partial pressure of dihydrogen (20%) after the complex has been sublimated under helium and just before the gaseous mixture is admitted to the fluidized bed.

In catalysis the purity of the metal is known to be of great importance and thus we focused our attention on the presence of heteroelements in the deposits. The effect of dihydrogen on purity was clearly evidenced (*vide infra*), because when a  $He/H_2$  gas mixture was used with **1** only traces of chlorine were found in the rhodium deposited on the surface or in the bulk of the supports. In contrast, when He alone was used, around one chlorine atom per rhodium atom was detected by energy dispersion spectroscopy (EDS), *vide infra*. Precursors **2** and **3** give rise to deposits containing large amounts of carbon and the presence of dihydrogen dramatically reduces these amounts (*vide infra*). Such a phenomenon has already been reported (23–25).

Thus, all subsequent experiments have been carried out in the presence of dihydrogen. Depending on the nature of the precursors, the sublimation has been carried out between 40 and  $55^\circ C$  and the decomposition in the fluid-

TABLE 1  
Characterization of the Rhodium Deposits

wt% Rh	Particle size (nm)	Dispersion	Specific surface area ( $\text{m}^2 \cdot \text{g}^{-1}$ )	Porosimetry ( $\text{cm}^3 \cdot \text{g}^{-1}$ )
0 <sup>a</sup>	—	—	170	315
0.35 <sup>b</sup>	1.1 <sup>c</sup>	0.97	184	
0.5 <sup>b</sup>	1.2 <sup>c</sup>	0.91	—	
1.0 <sup>b</sup>	1.4 <sup>c</sup> , 1.7 <sup>d</sup> , 1.8 <sup>c</sup>	0.78	178	289
2.0 <sup>b</sup>	1.5 <sup>c</sup>	0.71	172	
1.0 <sup>f</sup>	1.5 <sup>c</sup>	0.71	158 <sup>g</sup>	

<sup>a</sup> Pure silica.

<sup>b</sup> From  $[\text{Rh}_2(\mu\text{-Cl})_2(\text{CO})_4]$ .

<sup>c</sup> By CO chemisorption measurements.

<sup>d</sup> Determined by TEM.

<sup>e</sup> From  $\text{H}_2$  chemisorption measurements.

<sup>f</sup> From  $[\text{Rh}(\eta^3\text{-C}_3\text{H}_5)_3]$ .

<sup>g</sup> This silica powder has a specific area of  $149 \text{ m}^2 \cdot \text{g}^{-1}$ .

ized bed between 80 and 100°C, under a dynamic total pressure of 100 Torr.

#### Rhodium Deposition on Silica Powders

Representative supports used in this work were silica powders that had been sieved to give particle sizes between 100 and 200  $\mu\text{m}$ ; these samples were characterized by a density of 0.23 (B group of Geldart's classification (26)) and a BET area of  $170 \text{ m}^2/\text{g}$ . The grains of silica are spherical in shape, as shown by SEM observations (shape factor  $\approx 1$ ). We found a compressibility factor of 83, which shows that the silica powders are suitable supports for preparing catalysts and for carrying out fluidized bed experiments. The minimum fluidization velocity ( $U_{\text{mf}}$ ) was experimentally determined to be  $5.2 \text{ cm min}^{-1}$ . In order to have a good contact between the solid and the gas phase and to ensure a good homogeneity of the deposits, a bubbling regime was chosen with a fluidization velocity  $8 \times U_{\text{mf}}$ . The best compromise between the fluidization and the partial pressure of the organometallic precursor was found to be 50 Torr for the required dynamic reduced pressure. The flow rate of the carrier gas was adjusted to around 40 sccm to which, depending on the precursor, a 2- to 10-sccm flow of dihydrogen was added. Under these conditions, for compounds **1**, **2**, and **3**, the sublimation temperatures were 53, 40, and 55°C and the deposition temperatures were 100, 80, and 100°C, respectively. All these experiments were carried out for 2–5 h to obtain 0.3 to 2% (w/w) of rhodium on silica. The amount of rhodium deposited is directly proportional to the duration of deposition.

#### Characterization of the Supported Rhodium Catalysts

The particle sizes were determined indirectly by chemisorption of carbon monoxide or dihydrogen and directly

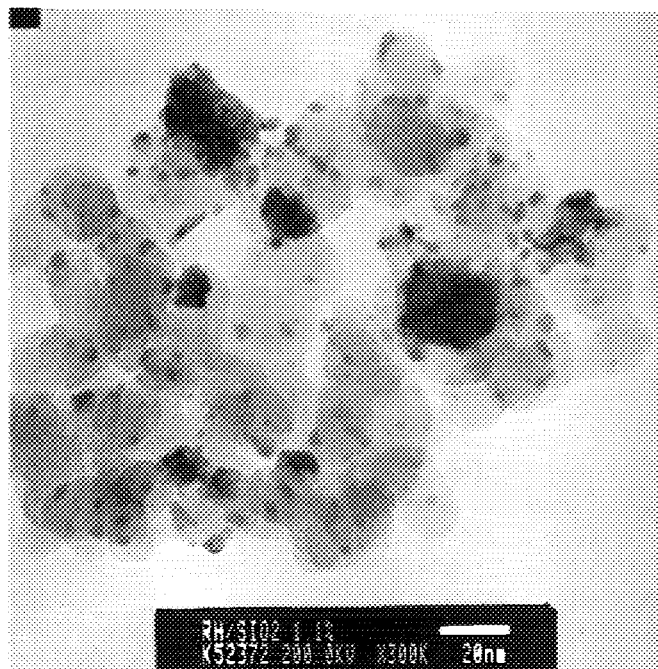


FIG. 2. Transmission electron micrograph of a 1% Rh/SiO<sub>2</sub> deposit issued from complex **1**.

by transmission electron microscopy. The isotherms of chemisorption for CO were measured at 298 K. The generally accepted stoichiometry of 1/1 for CO/Rh was assumed when the equilibrium pressure is reached.

The amounts of rhodium on the support and the metal particle sizes, dispersions, specific areas, and porosities thus obtained are displayed in Table 1. It can be seen that, by allowing the support to react with small amounts of precursor, low loadings can be obtained, leading to particularly small particles and therefore to an excellent dispersion. Loading the support with more rhodium produces larger particles but up to 2% Rh/SiO<sub>2</sub> the dispersion remains at 0.7. It is worth noting that there is no decrease in the specific surface area, showing that the porosity of the support is not affected by this process of deposition.

In order to visualize directly the rhodium particles, TEM was used for 1% Rh/SiO<sub>2</sub> deposits. Micrographs (Fig. 2) show that the particle sizes range from 1 to 3 nm (90% of the particles < 3 nm), with a distribution centered between 1 and 2 nm. Moreover, these deposits (from **1**) were compared to those prepared by conventional impregnation methods using  $\text{RhCl}_3 \cdot 3\text{H}_2\text{O}$ . After a reduction step at 200°C for 12 h, TEM/EDS analyses of these latter catalysts showed that chlorine still remains in the rhodium particles, with the atomic Cl/Rh ratio being very near 1; the particle sizes are around 3 nm.

X-ray diffraction spectra of a 3% Rh/SiO<sub>2</sub> powder with

TABLE 2

Relative Amounts of Rh, Cl, and C on the Deposits  
Determined by XPS (wt%)

Metal complex	Deposition conditions	% Rh	% Cl	% C
[Rh <sub>2</sub> Cl <sub>2</sub> (CO) <sub>4</sub> ]	He	77	23	—
	He/H <sub>2</sub>	98.5	1.5	—
[Rh(allyl) <sub>3</sub> ]	He	81	—	19
	He/H <sub>2</sub>	93	—	7
[Rh(CO) <sub>2</sub> (acac)]	He	68	—	32
	He/H <sub>2</sub>	86	—	14

larger particle sizes (3 nm) revealed the main crystallographic planes of metallic rhodium.

In order to obtain significant results on the chemical purity of the deposits, rhodium was deposited on planar bulky substrates under the above-mentioned experimental conditions. By SEM, it clearly appears that homogeneous films were formed with grain sizes ranging from 200 to 300 nm under helium, to 100 nm under He/H<sub>2</sub>. By EDS, the presence of rhodium was shown clearly. In the deposits resulting from **1**, and from **2** or **3**, chlorine and carbon respectively were observed qualitatively; the intensity of these signals decreased markedly when dihydrogen was added to the carrier gas.

Further analyses were carried out by X-ray photoelectron spectroscopy. Rhodium was shown to be metallic, the binding energies  $E(3d_{5/2}) = 307.1$  eV and  $E(3d_{3/2}) = 312.0$  eV being in good agreement with the literature data (27). When chlorine is present in the deposits, the two rhodium peaks become wider. A deconvolution revealed that rhodium is present in both zero [ $E(3d_{5/2}) = 307.4$  eV;  $E(3d_{3/2}) = 312.0$  eV] and III oxidation states [ $E(3d_{5/2}) = 308.8$  eV;  $E(3d_{3/2}) = 313.6$  eV]. Chlorine was detected at  $E(2p_{3/2}) = 197.9$  eV and  $E(2p_{1/2}) = 199.1$  eV; these values are consistent with terminal rhodium–chlorine bonds rather than bridging rhodium–chlorine bonds (28). Thus, chlorine could be present as RhCl<sub>3</sub> entities, in addition to metallic rhodium. Previous examinations of the pyrolysis products of [Rh<sub>2</sub>Cl<sub>2</sub>(CO)<sub>4</sub>] by Kumar and Puddephatt (19) have shown the presence of RhCl<sub>3</sub>.

Concerning precursors **2** and **3** which can lead to carbon incorporation in the deposits, whatever the presence or not of dihydrogen, the binding energy [ $E(1s) = 284.5$  eV] is consistent with a graphitic carbon.

Table 2 displays the semiquantitative results of the XPS analyses related to the various deposits obtained from precursors **1–3** with or without dihydrogen. The role of dihydrogen is unambiguously demonstrated, since for instance from **1**, only traces of chlorine can be detected. It is worth mentioning that under H<sub>2</sub> chlorine is more easily removed from **1** than carbon is removed from precursors **2** and **3**.

### Catalytic Tests

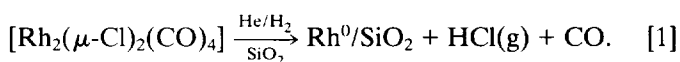
Owing to the small particle sizes obtained by this OMCVD method, the activity of these catalysts was examined in the classical hydrogenation reaction of alkenes and more especially of benzene, since this latter reaction is known to be structure sensitive for supported rhodium catalysts (29). The hydrogenation of oct-1-ene at 50°C under 0.1 MPa of dihydrogen led to an activity of 1170 mol·g<sub>Rh</sub><sup>-1</sup>·h<sup>-1</sup> for the 1% Rh/SiO<sub>2</sub> sample prepared from **1** or **2**, whereas a 1% Rh/SiO<sub>2</sub> sample obtained by the impregnation method gave 750 mol·g<sub>Rh</sub><sup>-1</sup>·h<sup>-1</sup>. This activity was found to be the same for three additional runs. Benzene was selectively hydrogenated into cyclohexane at 2 MPa and 85°C; the two catalysts gave activities of 140 and 85 mol·g<sub>Rh</sub><sup>-1</sup>·h<sup>-1</sup>, respectively.

In addition to the dispersion parameters which are generally lower for conventional catalysts, the greater activity in hydrogenation observed for the present catalysts is presumably due to the low amounts of chlorine (1.5 wt%).

### Approach to the Mechanisms

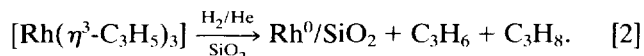
Preliminary investigations on the mechanism of this OMCVD process have been carried out using different techniques. On-line analyses of the decomposition products have been performed by coupling the CVD reactor with a mass spectrometer.

In an attempt to determine the influence of the gas mixture on the products of pyrolysis, an IR gas cell was charged with the various starting components and heated gradually. Under a helium atmosphere, complex **1** produces carbon monoxide at temperatures above 125°C and a solid characterized by a Rh/Cl ratio near 1. In contrast to previous reports (19) carried out at 180°C, no phosgene was detected even at 200°C. The absence of phosgene was confirmed by mass spectrometry. However, when dihydrogen is added to helium (about 20% vol/vol), above 75°C the loss of CO appears in a first step followed by the formation of HCl in the gas phase. As already noted, the solid deposit contains metallic rhodium with only traces of chlorine. The on-line mass spectrometry measurements show that in the presence of silica, CO, then immediately HCl are detected from a 1/H<sub>2</sub>/He mixture. Thus the results of the pyrolysis are summarized as

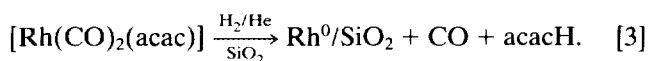


Decomposition of **2** leads to propene and 1,5-hexadiene under pure helium and to propene/propane mixtures under a H<sub>2</sub>/He atmosphere, as analyzed both by infrared and mass spectrometry. The presence of 1,5-hexadiene was not observed under a H<sub>2</sub> atmosphere, in contrast to what can

be expected from the results of Kumar and Puddephatt (19). Moreover, the presence of dihydrogen allows us to reduce dramatically the amounts of graphitic carbon in the deposit while simultaneously producing propane, the amounts of which are directly proportional to the quantities of  $H_2$ . The balance of our analyses is given by

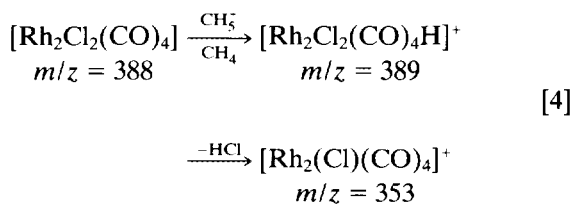


Under helium, the decomposition of complex **3** gives rise to CO, CO<sub>2</sub>, acetone, and butanone. Complex **3** heated under  $H_2/He$  (85°C) leads first to a loss of CO then to the formation of acetylacetone (2,4-pentanedione). The result of this decomposition is shown by



During all our infrared investigations no rhodium intermediate species were detected. Under a deuterium/helium atmosphere in the case of precursor **1** only CO and DCl loss have been analyzed.

In addition, further studies on complex **1** by chemical ionization mass spectrometry using methane showed the presence of the quasi-molecular fragment  $m/z = 389$  ( $^{35}Cl$  isotope), and by loss of HCl the fragment  $m/z = 353$ :



Thus, although the reaction conditions are not strictly comparable, complex **1** can be protonated in the gas phase to give an intermediate species which easily loses HCl.

However, the presence of the first rhodium atoms deposited on the support plays an important role in the course of the CVD. Indeed, during an experiment carried out at 80°C and followed by mass spectrometry, the supply of dihydrogen was stopped after a period of about 1 h. For more than 20 min, HCl was detected, although its amounts were decreasing. In the absence of dihydrogen in the carrier gas, HCl can only be formed from hydrogen present on the support and presumably from rhodium-hydride species. We have determined that in the absence of dihydrogen, the decomposition of **1** does not produce any HCl, which could occur if surface silanols would react. In addition, whereas rhodium deposits usually occur on silica in the fluidized bed and not on the walls of the reactor, an experiment was carried out in the absence of silica to de-

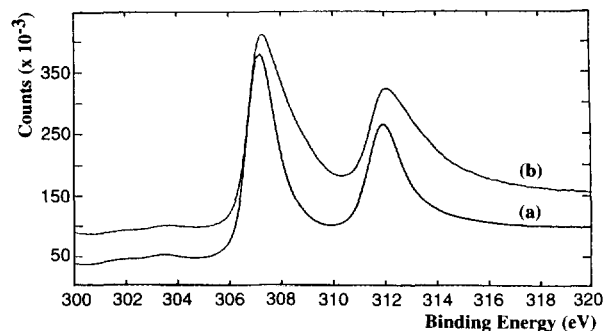


FIG. 3. XPS spectra of rhodium deposited on a planar  $SiO_2$  substrate, after etching by  $Ar^+$  for (a) 5 and (b) 20 min. The figure shows the Rh 3d region.

posit a little rhodium on the walls. Further addition of silica and then deposition of rhodium under the standard conditions resulted in the preferential growth of the deposit on the walls going on, and to a small extent, to the expected one on  $SiO_2$ . Such a phenomenon has already been observed by Xue *et al.* in the case of chemical vapor deposition of platinum from the complex  $[(MeCp)PtMe_3]$  on different kinds of surfaces (23).

Finally, we can propose that in the gas phase, reactive species are formed resulting from the loss of CO and/or HCl from complex **1**. These species interact with particular sites of the support, giving rise to the first rhodium anchoring. A second simultaneous mechanism can occur which involves the active participation of rhodium-hydride species on metal particles. Such rhodium-hydride species have already been reported by Fischer *et al.* (30).

Recently Dufour *et al.* (31) have studied the reaction of complex **2** at room temperature with various pretreated supports; it was shown that the surface reacts through OH groups to afford a rhodium-oxygen bond with elimination of an allyl ligand as propene. However, in the present study, active intermediate species are formed in the gas phase, due to the presence of dihydrogen, which do not require OH groups to anchor to the support. The more surface area is disposable, the faster is the phenomenon.

In order to have an insight into what kind of interaction occurs between the support and the first incoming rhodium intermediate species, XPS studies have been carried out. A very thin film of rhodium was deposited on a planar silicon substrate coated with a 20-nm-thick silicon oxide layer. XPS spectra were recorded after successive etching operations by  $Ar^+$  ion bombardment of the rhodium film (Fig. 3). Spectrum **a** recorded after 5 min etching, is representative of metallic rhodium with binding energies of  $3d_{5/2}$  at 307.0 eV and  $3d_{3/2}$  at 311.9 eV. Further etching resulted in the two peaks broadening, as shown in spectrum **b**. Careful deconvolution of these two signals (Fig. 4) showed the presence of rhodium in the zero oxidation state (at 307.0 and 311.9 eV), and in the +I and +III oxidation states. Indeed, the two peaks at 308.0

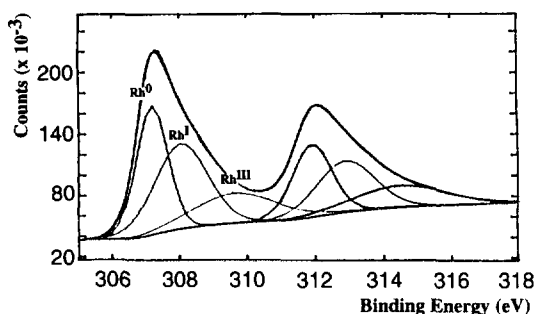


FIG. 4. Deconvolution of the XPS curves in the Rh 3d region of interest.

and 312.9 eV are consistent with Rh(I) species and the two broad peaks at 309.6 and 314.4 eV correspond to Rh(III), as compared to the  $3d_{5/2}$  energies quoted between 308.8 and 311.3 eV (27).

Thus, the anchoring of rhodium on the surface involves covalent bonds between rhodium and oxygen atoms originated from silica. Rh(I)-O- and Rh(III)(-O-)<sub>3</sub> bonds have been evidenced in this work. Previous studies on rhodium complexes adsorbed on alumina (32) or silica (33) have shown that Rh(I) and Rh(III) surface atoms are bonded to oxygen atoms of the support.

### CONCLUSION

The one-step method described here coupling OMCVD and a fluidized bed provides a rapid way to prepare at low temperature highly dispersed rhodium aggregates anchored on the support. Such catalysts present good catalytic activities in hydrogenation.

Further work to examine catalytic performance in carbonylation reactions are in progress.

### ACKNOWLEDGMENTS

This work was mainly supported by the European Economic Community through the BRITE-EURAM programme BREU-CT 91-0458 and by the Région Midi-Pyrénées, which are gratefully acknowledged. Thanks are due to our colleagues involved in this programme for several characterizations of the deposits and helpful discussions: A Kiennemann and L. Chateau (EHICS, Strasbourg), C. Mazzocchi (Politecnico di Milano), J. P. Guerlet, N. Petit, and M. Malheiro (Comptoir Lyon-Alemand-Louyot, Paris). We are indebted to A. Reynes (ENSC, Toulouse) for carrying out the mass spectrometry experiments and to P. Tobaly for carrying out the vapor pressure measurements (LIMHP-CNRS, Villeta-neuse). We thank also our colleagues in Chemical Engineering for helpful advice in the design of the reactor: J. P. Couderc (ENSIGC, Toulouse) and J. Molinier (ENSC, Toulouse).

### REFERENCES

- Gurav, A. S., Duan, Z., Wang, L., Hampden-Smith, M. J., and Kodas, T. T., *Chem. Mater.* **5**, 214 (1993).
- Duan, Z., and Hampden-Smith, M. J., *Chem. Mater.* **5**, 994 (1993).
- Arai, M., Vsui, K. I., and Nishiyama, Y., *J. Chem. Soc. Chem. Commun.*, 1853 (1993).
- Fernandez, A., Gonzalez-Elipe, A. R., Cabellero, A., and Munuera, G., *J. Phys. Chem.* **97**, 3350 (1993).
- Pocard, N. L., Alsmeyer, D. C., McCreery, R. L., Neenan, T. X., and Callstrom, M. R., *J. Am. Chem. Soc.* **114**, 769 (1992).
- Fernandez, A., Gonzalez-Elipe, A. R., Real, E., Cabellero, A., and Munuera, G., *Langmuir* **9**, 121 (1993).
- Fernandez, A., Munuera, G., Gonzalez-Elipe, A. R., and Espinos, J. P., *Appl. Catal.* **57**, 191 (1990).
- Serp, Ph., Feurer, R., Morancho, R., and Kalck, Ph., *J. Mol. Catal.* **101**, L107 (1995).
- Dossi, C., Bartsch, A., and Losi, P., "Advanced Syntheses and Methodology in Inorganic Chemistry" (S. Daolio, Ed.), p. 83, 1991.
- Dossi, C., Bartsch, A., Fusi, A., Sordelli, L., Ugo, R., Bellatreccia, M., Zanoni, R., and Vlais, G., *J. Catal.* **145**, 377 (1994).
- Omata, K., Mazaki, M., Yagita, H., and Fujimoto, K., *Catal. Lett.* **4**, 123 (1990).
- Köhler, S., Trautmann, S., Dropsch, H., and Baerns, M., Abstracts, Europacat-I (Montpellier, France, 1993), p. 428.
- Powell, J., and Shaw, B. L., *J. Chem. Soc. A*, 583 (1968).
- Varshavskii, Yu. S., and Cherkasova, T. G., *Russ. J. Inorg. Chem. Engl. Transl.* **12**, 899 (1967).
- Deeming, A. J., and Sharrat, P. J., *J. Organomet. Chem.* **99**, 447 (1975).
- Tobaly, P., *Rev. Sci. Instrum.* **62**, 2011 (1991).
- Hindermann, J.-P., Hutchings, G. J., and Kiennemann, A., *Cat. Rev.-Sci. Eng.* **35**, 1 (1993).
- Boujana, S., Demri, D., Cressely, J., Kiennemann, A., and Hindermann, J.-P., *Catal. Lett.* **7**, 359 (1990).
- Kumar, R., and Puddephatt, R. J., *Can. J. Chem.* **69**, 108 (1991).
- Smith, D. C., Patillo, S. G., Elliot, N. E., Zocco, T. G., Laia, J. R., and Sattelberger, A. P., in "C.V.D.—XI. Proceedings of the Eleventh International Conference," (Spear, K. E., and Cullen, G. W., Eds.), p. 610. The Electrochemical Society Inc., Pennington, NJ, 1990.
- Flist, E. B., Messelhauser, J., and Suhr, H., *Appl. Surf. Sci.* **54**, 56 (1992).
- Kaes, H. D., Williams, R. S., Hicks, R. F., Zink, J. I., Chen, Y. J., Müller, H. J., Xue, Z., Xu, D., Shuh, D. D., and Kim, Y. K., *New J. Chem.* **14**, 527 (1990).
- Xue, Z., Strouse, M. J., Shuh, D. K., Knobler, C. B., Kaesz, H. D., Hicks, R. H., and Williams, R. S., *J. Am. Chem. Soc.* **111**, 8779 (1990).
- Kaplin, Y. A., Belysheva, G. V., Zhilt'sov, S. F., Domrachev, G. A., and Chernyshova, L. S., *J. Gen. Chem. USSR Engl. Transl.* **50**, 100 (1980).
- Xue, Z., Thridandam, H., Kaesz, H. D., and Hicks, R. F., *Chem. Mater.* **4**, 162 (1992).
- Geldart, D., *Powder Technol.* **7**, 285 (1973).
- Wagner, C. D., Riggs, W. M., Davis, L. E., Moulder, J. F., and Muilenberg, G. E., "Handbook of X-Ray Photoelectron Spectroscopy" (Muilenberg, G. E., Ed.), p. 108. Perkin-Elmer Corp., Eden Prairie, MN, 1987.
- Ebner, J. R., McFadden, D. L., Tyler, D. R., and Walton, A., *Inorg. Chem.* **15**, 3014 (1976).
- Graydon, W. F., and Langan, M. D., *J. Catal.* **69**, 180 (1981).
- Fischer, H. E., King, S. A., Miller, J. B., Ying, J. Y., Benziger, J. B., and Schwartz, J., *Inorg. Chem.* **30**, 4403 (1991).
- Dufour, P., Houtman, C., Santini, C. C., Nèdez, C., Basset, J. M., Hsu, L. Y., and Shore, S. G., *J. Am. Chem. Soc.* **114**, 4248 (1992).
- Bowser, W. M., and Weinberg, W. H., *J. Am. Chem. Soc.* **103**, 1453 (1981).
- Foley, H. C., Decanio, S. J., Tau, K. D., Chao, K. J., Onuferko, J. H., Dybowski, C., and Gates, B. C., *J. Am. Chem. Soc.* **105**, 3074 (1983).